High Energy-High Repetition Rate Fiber Laser System for Precision Micromachining with Fundamental and Second Harmonic Wavelengths

Fumiyo YOSHINO*, James BOVATSEK*, Alan ARAI*,
Yuzuru UEHARA**, Zhenlin LIU** and Gyu CHO**

*IMRA America, Inc. Applications Research Laboratory
48834 Kato Road, Suite 106A, Fremont, CA 94538 U.S.A.
E-mail: fyoshino@imra.com
** IMRA America, Inc.
1044 Woodridge Avenue, Ann Arbor, Michigan 48105 U.S.A.

Interest in femtosecond laser micromachining has been growing for applications that require precise material removal or modification over very small features. Flat panel display manufacturing, lithography mask repair, semiconductor wafer scribing and optical waveguide writing are some examples where femtosecond pulse lasers are being studied. IMRA's latest experimental prototype FCPA is based on components similar to the production FCPA *μJewel* D-400. The latest design concept produces 10-μJ pulses at a repetition rate of up to 100 kHz or 1-μJ pulses at 1 MHz using Yb-doped fiber amplifier technology. Frequency-doubling produces 522-nm wavelength output with pulse energies up to 4 μJ. The higher pulse energy, relatively high repetition rate, availability of efficient frequency-doubling with a compact, reliable design will enable additional industrial applications. This paper describes the experimental results comparing the nonlinear optical loss through different types of transparent materials. The combination of the nonlinear absorption initiated by the ultrashort pulses and the heat accumulation from the high repetition rate enable some unique advantages over other lasers. The effect of the two different wavelengths (1045 nm and 522 nm) on processing of transparent materials is illustrated in several examples.
DOI: 10.2961/jlmn.2006.03.0021
Keywords: femtosecond, ultrafast, micromachining, silicon, sapphire, glass, laser scribing

1. Introduction

Interest in femtosecond micromachining of continues to increase, due in large part to transparent material processing applications. The high peak intensity of ultrashort pulses enables efficient nonlinear absorption in transparent media [1]. This allows unique processing capabilities, such as precise 3D machining inside the bulk of transparent materials for optical waveguide fabrication and welding of transparent materials [2-4].

IMRA's FCPA *μJewel* offers a combination of high pulse energy and high repetition rate operation. High energy allows for a larger amount of material removal by ablation. High repetition rate contributes to faster processing time in industrial manufacturing.

IMRA's 10μJ prototype FCPA *μJewel,* has been tested for several micromachining applications including ITO removal [5] and scribing of sapphire wafers and borosilicate glass substrates (for Liquid Crystal Display (LCD)) [6]. In this paper, we present our most recent experimental results comparing laser micromachining with the fundamental at 1045 nm and its frequency doubled light at 522 nm.

2. Micro-Joule Femtosecond Fiber Laser

The laser used in the experiments is based on fiber-stretched pulse amplification with a large area core Yb-doped fiber, incorporating non-linear optical phase control in the fiber [7]. The emission wavelength is 1045 nm. This compact design (550x400x131mm^3, weighing about 25 kg) has been shown over the last several years to be an excellent choice for realizing a robust, true turn-key femtosecond laser with micro-joule level pulse energy for daily use. Recently we have successfully reconfigured the design as a commercial product for the generation of amplified pulses with energy up to 10 μJ while maintaining femtosecond pulse recompressibility.

The basic design of the amplifier is based on a femtosecond Yb-fiber oscillator followed by a fiber stretcher and amplifier chain including a large area fiber with an Yb-doped core excited by cladding pumping. A grating compressor recompresses the amplified pulse. The repetition rate initially determined by the oscillator is about 50 MHz and is reduced for high pulse energy amplification by an acousto-optic modulator to between 100 kHz and 5 MHz (50 kHz in the experimental setup). A key advantage is the lack of high-voltage components in the system, in contrast to a Pockels cell. All critical components are linked with fiber-optics, so the robustness and reliability are incomparable to a solid-state based system with similar performance parameters.

Fig. 1 shows a typical auto-correlation function of pulses with energy of 10 μJ at a repetition rate of 100 kHz. The typical pulse duration is about 500 fs assuming a sech^2-pulse. As clearly shown in the plot, most of the energy is contained within the assumed pulse shape. It is worth noting that the pedestal present in an auto-correlation measurement is exaggerated due to the nature of the convolution of two pulses over the delay time in the auto-correlation function. The beam profile shown in the inset

has a typical ellipticity of less than 10% based on a Gaussian fit of the transverse mode, demonstrating the high beam quality. A novel technique to guide and amplify the fundamental mode in a large area fiber core has been implemented in the power amplifier design [8].

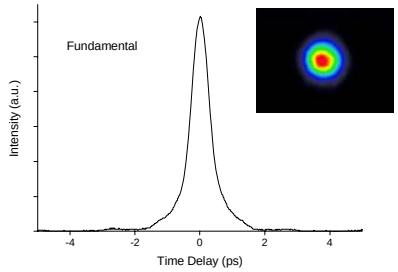

Fig. 1 Typical pulse form of auto-correlation function of 10 μJ pulses at 100 kHz. The inset shows the beam profile.

The capability of the laser to generate high pulse energy at a repetition rate in the MHz range is a very attractive feature for many applications where, for instance, process speed is critical. Our laser can be tuned to a repetition rate of 1 MHz with pulse energy at the 1-μJ level. Fig. 2 shows an auto-correlation function of 1.3 μJ-pulses running at 1 MHz.

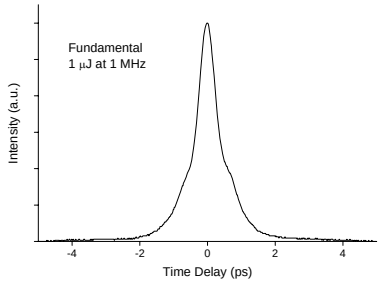

Fig. 2 Typical pulse form of auto-correlation function of 1 μJ pulses at 1 MHz.

For the data in Figs. 1 and 2, we have changed only the dispersion in the pulse compressor in our experimental prototype. The auto-correlation function in Fig. 2 shows higher intensity in the pedestal, which is characteristic of the nonlinear pulse compression based on the cubicon concept [7]. Lower energy pulses are not necessarily more compressible than higher energy pulses, distinguished from conventional linear chirped pulse amplification. Note that non-linear phase compensation in the gain fiber is optimized for 10 μJ in our amplifier. Nevertheless the pulse duration in Fig. 2 is well below 1 ps. Both auto-correlation functions were measured with a commercial system (APE Pulse Check).

3. Second Harmonic Generation (SHG)

The second harmonic wavelength (522 nm) was generated by a non-critically phase matched (NCPM) LBO crystal. This crystal was chosen for its high conversion efficiency and ease of alignment with different focusing optics, which are necessary for the various repetition rates of the FCPA *μJewel*. The setup is shown below.

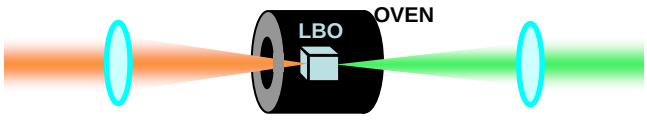

Fig. 4 Setup for SHG with LBO crystal.

The conversion efficiency was about 50% with a 250-mm focal length lens. The optimized temperature was 173.7°C. This simple setup produces good beam quality with a symmetric Gaussian profile (Fig. 5). Spectra of the fundamental (FW) and second harmonic (SH) wavelengths are shown in Fig. 6.

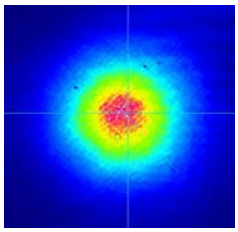

Fig. 5 CCD image of SHG beam profile

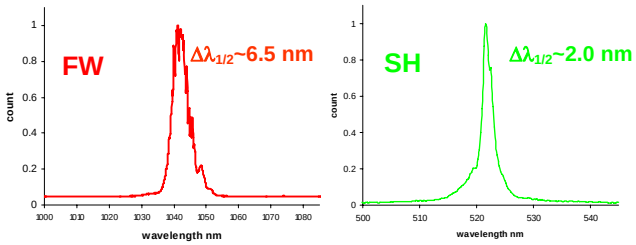

Fig. 6 Spectra of fundamental (FW) and second harmonic (SH) wavelengths

The second harmonic (SH) pulse width is expected to be as short as fundamental wavelength (FW) [9]. Most of the experiments with the second harmonic used the maximum pulse energy of ~4 μJ delivered at the target. The pulse energy was adjusted with an optical attenuator.

4. Comparison of Fundamental and Second Harmonic Wavelengths for Micromachining

Some materials have lower ablation thresholds with shorter wavelengths (Table 2 [10-11]). For some materials, the nonlinear process is more efficient at different wavelengths. A few laser micromachining examples are compared at the fundamental (1045 nm) and second harmonic (522 nm) wavelengths of the prototype 10 μJ FCPA.

Table 2 Material damage thresholds, J/cm^2 [10-11]

Material	1045 nm 100 kHz	522 nm 100 kHz
Gold	0.29	0.2
Silicon	0.099	0.066
Borosilicate	2.9	2.5
Sapphire	1.9	1.5
Fused Silica	2.9 (200 kHz)	
Copper	0.47 (200 kHz)	

4.1 Nonlinear loss ~ Fused Silica ~

(Received: May 16, 2006, Accepted: December 1, 2006)

Fabrication of low-loss optical waveguides in fused silica (Corning 7980) with the second harmonic wavelength has been demonstrated with FCPA *μJewel* D-400 system at 1 MHz [2]. With the same system, the fundamental wavelength did not produce low-loss waveguides. The difference may be due to the order of the nonlinear processes involved. As fused silica has a large bandgap, ~9 eV, more photons need to be absorbed simultaneously with the 1045 nm wavelength (~8 photons) than with 522 nm (~4 photons). There may be a lower limit to the wavelength dependence since others have reported less success when using 400 nm compared to 800 nm radiation [12].

We studied the difference in the nonlinear loss between the second harmonic and fundamental wavelengths. The setup used is similar to that of a Z-scan system [13]. In order to achieve a gradual variation of the input intensity, the sample was scanned in the propagation direction of the focused beam (Fig. 7). The power of the transmitted beam was measured at various distances from the focus (Fig. 8).

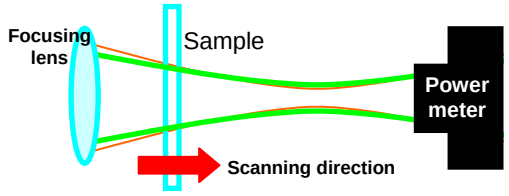

Fig. 7 Setup for nonlinear transmission measurement

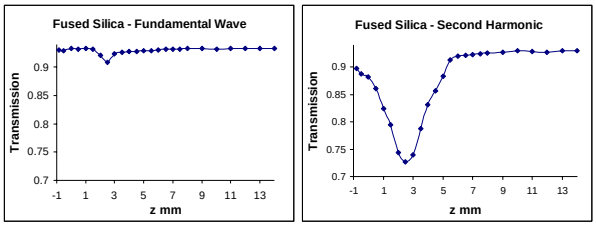

Fig. 8 Transmission through 1-mm thick fused silica

The numerical aperture (NA) is one of the more critical parameters which affect the damage threshold of transparent materials [14]. Lower NA makes the threshold higher since more pulse energy is then required to achieve the required intensity. In order to have similar beam diameters at the focus with both wavelengths, different focusing geometries were used for each wavelength. The resultant focus spot was slightly smaller with the fundamental wavelength. The focal spot diameters were about 42 μm and 50 μm for the fundamental and second harmonic, respectively. The calculated NA from the beam propagation was 0.039 for fundamental wavelength and 0.016 for second harmonic.

Despite the fact that the focusing geometry should promote a lower damage threshold with the fundamental wavelength, material modification occurred at lower pulse energies with the second harmonic. This indicates that the modification is much easier at 522 nm; light is absorbed more efficiently.

In addition to the damage threshold, with the fundamental wavelength there was a distinct range over which a nonlinear decrease in transmission was observed, but with the second harmonic the change from linear transmission to damage occurred abruptly. This may be due to the efficient absorption process which rapidly leads to avalanche photo-ionization.

This is a useful result not only for waveguide writing, but also for other processes of fused silica (quartz)/glass with ultrashort pulses. Figs. 9 and 10 show a comparison of static exposures at various repetition rates and number of pulses. Although the energy is the same in both cases, the material modification is much stronger with the second harmonic.

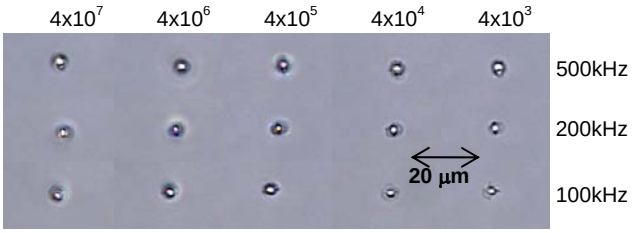

Fig. 9 Fused silica static exposure with the second harmonic wavelength (pulse energy~240 nJ ~NA0.65)

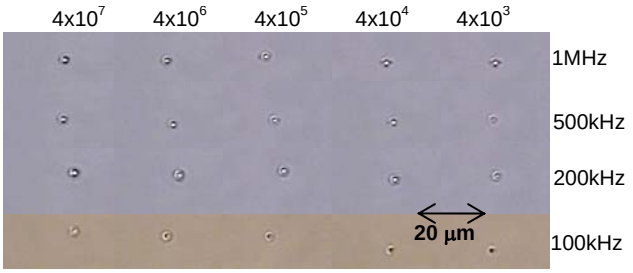

Fig. 10 Fused silica static exposure with the fundamental wavelength (pulse energy~240 nJ NA0.65)

4.2 Laser Scribing of Industrial Materials

The lower material modification threshold can help to efficiently remove material. Smaller features due to the shorter wavelength can also be an advantage.

Laser scribing of three industrially important materials was tested. These are materials which have increasing interest for precision micromachining. As the thickness of the wafer or substrate becomes thinner, higher precision is required. Femtosecond laser processing could be the solution.

4.2.1 Silicon wafer

Silicon wafers are becoming thinner and more difficult to scribe or dice with conventional diamond blade technology. Thin wafers are more fragile, so a slower speed is required to achieve good cut quality. Ultrashort pulse laser scribing may offer a solution to overcome the difficulties with blades (chipping and crack).

The efficiency of femtosecond pulse machining of silicon is higher with a wavelength of 400 nm compared to 800 nm [15]. We have compared 10 μJ-1045 nm and its frequency doubled light, 4 μJ-522 nm, for silicon scribing.

Perpendicular polarization (with respect to the scanning direction) has been shown to produce a higher quality cut geometry [16]. From the cross-sectional image, the material removal itself seems to be more efficient with perpendicular polarization (Fig. 11).

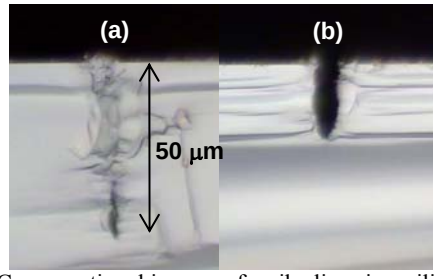

Fig. 11 Cross-sectional images of scribe lines in a silicon wafer by fundamental wavelength; polarization parallel (a) perpendicular (b) to the scanning direction.

With polarization parallel to the scanning direction, the scribe depth can be as deep as 50 μm, twice as deep as with perpendicular polarization with the same pulse energy and scanning speed (20 mm/s). The width of surface modification was ~12 μm. The scribed feature appears more open in the case with perpendicular, whereas much deeper inner material modification can be seen with parallel polarization. The effect of polarization for both second harmonic and fundamental wavelengths is similar.

With the second harmonic maximum energy of 4 μJ, the deepest scribe line with parallel polarization at the speed of 20 mm/s was ~40 μm, with a surface scribe width of ~10 μm. The scribing efficiency (depth per unit energy) is higher with the second harmonic wavelength than with the fundamental, with which 30 μm was scribed with 5 μJ at the same speed.

Different scribe cross-sectional shapes are possible with different wavelengths. With polarization perpendicular to the scan direction, the second harmonic wavelength gives a narrower, cleaner scribe, where the fundamental produces a rounder shape.

4.2.2 Sapphire wafer

Sapphire wafers are commonly used as blue LED substrates. In our previous tests, the "dual scribe" method (simultaneous machining of both a surface groove and a separate bulk modified region) resulted in a faster scan speed with the fundamental wavelength [6]. Similar to fused silica, sapphire has one of the highest bandgaps among transparent materials. As the wavelength approaches UV, there is a monotonic increase in the nonlinear coefficient [17]. Because the nonlinear process is required to initially absorb light in transparent materials, it is natural to expect a large difference in machining sapphire with the fundamental and second harmonic wavelengths. Fig. 12 shows the surface scribe depth as a function of scanning speed.

The depth of the surface scribe with 4-μJ of the second harmonic was similar to what was possible with the 10-μJ at the fundamental wavelength [6]. Although the damage threshold is about 25% lower with the second harmonic, the 60% difference in pulse energy is too large to overcome. The width of the surface scribe lines were less than 5 μm at all the speeds tested.

When the focus position is deeper into the material, inner modification was observed. As was seen with the fundamental beam [6], with the focal position a few 10's of μm deeper into the material, dual scribe lines were fabricated in sapphire.

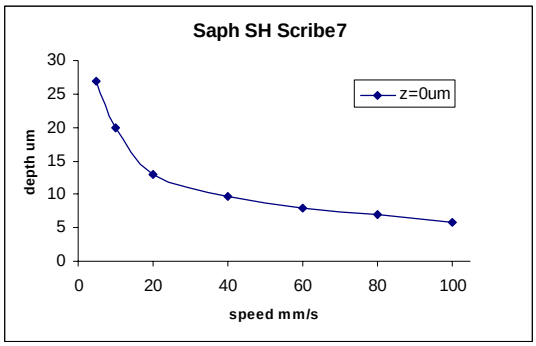

Fig. 12 Sapphire surface scribe depth at various scan speeds using the second harmonic wavelength (522 nm).

In addition, when the focus position with the second harmonic wavelength is much deeper into the material, there were cases where only inner material modification was produced. This may be due to the higher absorption of the light with the shorter wavelength providing higher photon energy. The extent of the modified area is more than half of the thickness of the 100-μm thick wafer. Despite the length of the modified area, it was difficult to break the sapphire wafer without a surface scribe. This led us to attempt applying higher intensity to this process by focusing the light tighter within the material. Fig. 13 shows cross-sectional images of modified sapphire using tighter focus (NA~0.27) when lowering the focus position from 15 μm above the surface (upper right) to 40 μm below the surface (lower left). The peak intensity increase was about 1.7 times the previous condition.

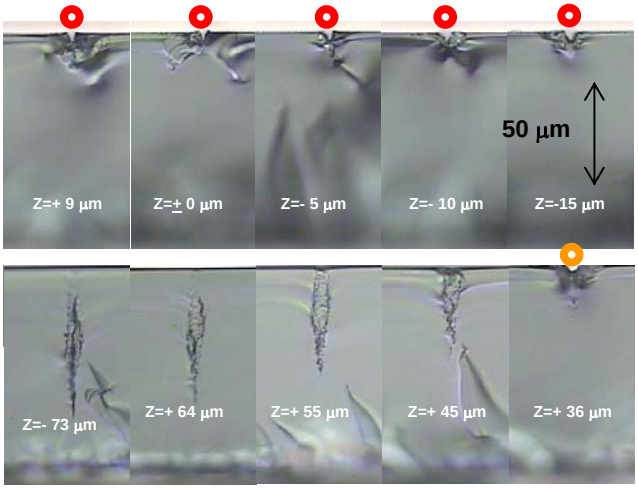

Fig. 13 Cross-sectional images of the modified area with increasing focus depth (30x aspheric lens, scan speed 40 mm/s). Z position indicates focal position with respect to the top surface. Red circles indicate conditions that produced a smooth surface cleave of 100-μm thick wafer.

Much stronger material modifications were observed with higher intensity. This resulted in more consistent breaking along the scribe lines when there is surface modification. However, it was still not possible to cleanly break the wafer without the surface scribe. Further increase of the intensity may help the breaking process. Also, with much tighter focusing, the fundamental wavelength could also yield inner modification of sapphire without the surface scribe.

(Received: May 16, 2006, Accepted: December 1, 2006)

4.2.3 Display glass substrate ~Corning 1737~

CO_2 lasers have been commonly used for scribing/dicing glass where high precision is not required. As thinner substrates are becoming more common, contributing to the reduction of the final product weight (e.g. cell phone, PDA and FPD), technology with higher precision is necessary.

We tested Corning 1737 which is used for active matrix liquid crystal display (LCD) cover glass. The scribe depth was found to be similar to our previous test with borosilicate glass using 10-μJ at the fundamental wavelength (Fig. 14) [6]. A scribe depth of about 50 μm was possible with 2.5-mm/s scan speed. The width of the scribe was ~7.5 μm at 2.5 mm/s and less for faster speeds.

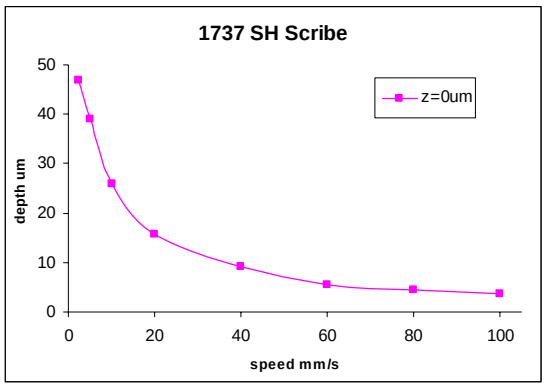

Fig. 14 Surface scribe depth at various scan speeds

Examples of cleave facets are shown in Fig. 15. Better quality cleave facets can be seen with deeper scribe lines.

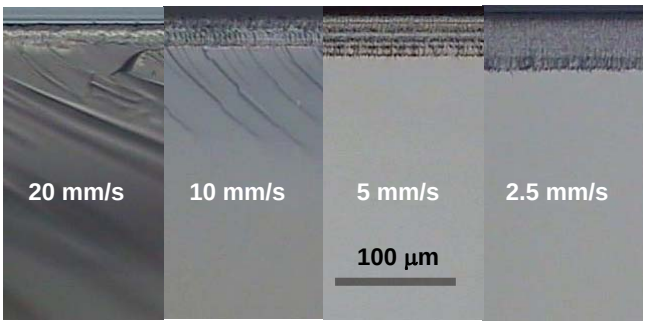

Fig. 15 Cleave facets with various scan speeds (1737 glass, t=1.1mm).

Similar to sapphire scribing, inner modification of the material was also observed in 1737 (Fig. 16). In comparison to sapphire scribing, the material modification is smoother, which is consistent with what has been seen in optical waveguide fabrication.

Although the inner material modification seems subtle, the dual scribe method made it possible to break 1.1-mm thick 1737 along the scribe line produced with a scan speed of up to 20 mm/s (Fig. 17). Higher pulse energy would help further increase the speed and allow breaking of even thicker material.

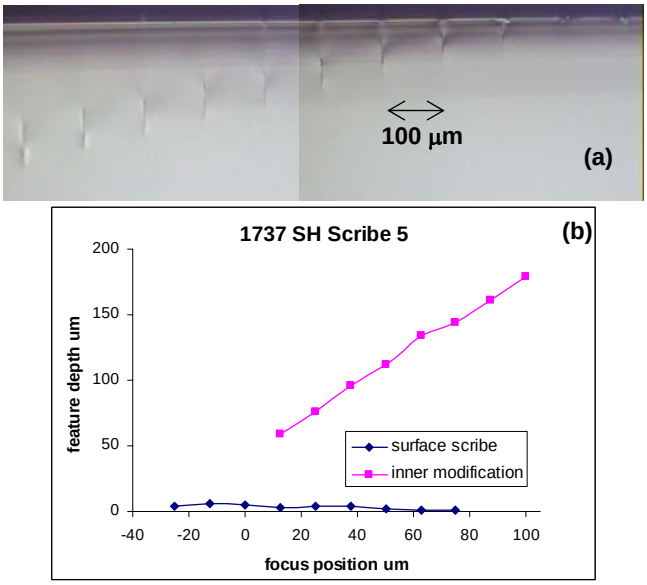

Fig. 16 Inner modification of 1737 **(a)** cross-sectional image **(b)** depth of modified area.

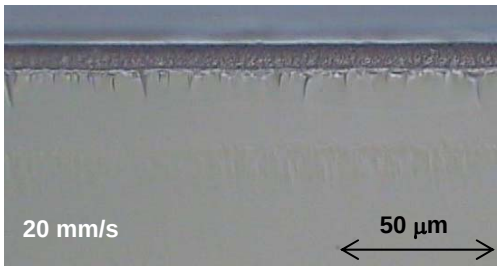

Fig. 17 Dual scribe cleave facet (1737 glass, t=1.1 mm)

4.2.4 Summary for the laser scribing

Using the second harmonic resulted in higher efficiency of material removal (per unit energy). Internal material modifications were observed with the second harmonic wavelength in sapphire and 1737 glass. Higher pulse energy is expected to further improve material scribing to consistently break wafers and substrates.

4.3 Groove cutting in Copper and Gold

Copper and gold have a large difference in their reflective properties at 1045 nm and 522 nm. Better laser machining with the 522 nm wavelength, such as marking and thin film removal, is well known [18]. Here, femtosecond laser groove cutting with these metals are compared.

A narrow, deep groove was cut in copper at a speed of 20 mm/s. The width of the groove was less than 20 μm and the depth was about 5 μm (Fig. 18-left). 4 μJ at the second harmonic was used with a 75-mm focal length lens. With the fundamental, 6 μJ was used with 40-mm focal length lens in order to fabricate similar feature dimensions. The difference in the amount of material re-deposition is significant. The groove cut with fundamental wavelength was accompanied by what appears to be oxidation.

The groove cut with the second harmonic seems very smooth in gold without any obvious modification of the material or debris re-deposition (Fig. 18-top right). In comparison to the case with second harmonic, debris re-deposition around the groove and the rougher groove bottom can be seen with fundamental.

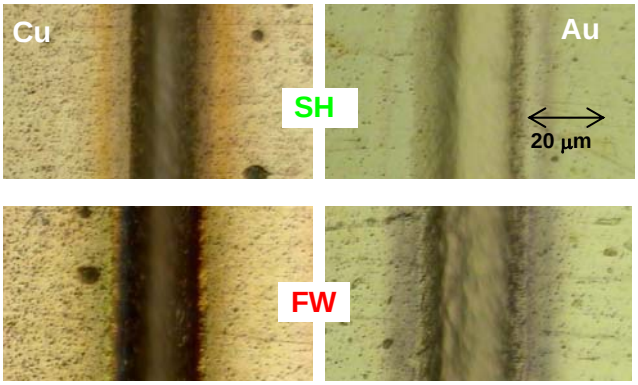

Fig. 18 Grooves in copper (depth ~5 μm) and gold (depth ~4 μm) with the second harmonic (SH, top) and fundamental (FW, bottom)

4.4 Laser Induced Periodic Surface Structure (LIPSS)

LIPSS is an interesting and possibly efficient method to fabricate periodic nano-texture on the surface of materials. Potential applications of surface nano-structuring include tribology (surface nano-reservoir for lubricant) and marking where shallow but clear contrast is needed [19].

LIPSS can be fabricated when the laser fluence is near the ablation threshold. Although the formation mechanism of these structure is not completely understood, the periodicity of the LIPSS, Λ, can be expressed as $\Lambda = \lambda / (n - \sin\theta)$, where λ=wavelength, θ=incident angle, n=effective refractive index. The microscope image (Fig. 19) shows LIPSS fabricated on nickel-coated plastic with the fundamental and second harmonic wavelengths. The feature periodicity is about the wavelength of the incident light. Variation of the wavelengths adds flexibility to nano-structure fabrication.

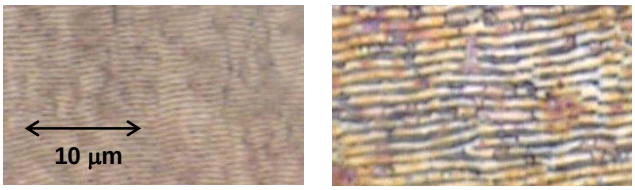

Fig. 19 LIPSS by second harmonic (left) and fundamental (right). Pulse energy 10 μJ, repetition rate 50 kHz, >10 pulses overlap

5. Summary

The second harmonic wavelength was generated using a simple setup with an LBO crystal in NCPM condition and the prototype 10 μJ FCPA system, delivering about 4 μJ of 522 nm energy at the machining target.

Several micromachining examples were discussed to show the difference between the fundamental and second harmonic wavelengths. For some cases the second harmonic showed better machining quality. More effective nonlinear absorption was observed in fused silica with the 522-nm wavelength due to the smaller number of photons involved in the absorption process.

Shorter wavelength offers tighter focus spot and a more elongated machinable focal volume. This was illustrated by the silicon scribing example. Scribing of wafers showed similar performance in the surface depth with fundamental wavelength. Inner modification without the surface scribe was possible with the second harmonic.

Cleaner groove cutting was demonstrated with the second harmonic wavelength in copper and gold. The second harmonic wavelength was also used in Laser Induced Periodic Surface Structures on metal surfaces yielding sub-micron periodicity.

In addition, we have observed that the polarization with respect to the scanning direction has a significant effect on the machining depth in silicon wafer.

Acknowledgments

The authors would like to acknowledge helpful discussions with Lawrence Shah and Donald Harter of IMRA America.

References

[1] B.C. Stuart, M.D. Feit, S. Herman, A.M. Rubenchik, B.W. Shore, and M.D. Perry: Phys. Rev. B, **53**, (1996) 1749.

[2] L. Shah, A.Y. Arai, S.M. Eaton, and P.R. Herman: Opt. Express, **13**, (2005) 1999.

[3] S. Eaton, H. Zhang, P. Herman, F. Yoshino, L. Shah, J. Bovatsek, and A. Arai: Opt. Express, **13**, (2005) 4708.

[4] J. Bovatsek, A. Arai, and C.B. Schaffer: CLEO/QELS Conference and PhAST Technical Digest (2006) CThEE6.

[5] D. Farson, H.-W Choi, K.-R Kim, and S.K. Hong: Int'l. Meeting on Information Display (2005) 583.

[6] J. Bovatsek, A. Arai, F. Yoshino, and Y. Uehara: "Fiber Laser III: Technology, Systems and Applications", Proc. of SPIE Vol. 6102-01 (2006).

[7] L. Shah, Z. Liu, I. Hartl, G. Imeshev, G.C. Cho, and M.E. Fermann, Opt. Express, **13**, (2005) 4717.

[8] M.E. Fermann, Opt. Lett. **23**, (1998) 52.

[9] SNLO nonlinear optics code available from A.V Smith, Sandia National Laboratories, Albuquerque, NM, http://www.sandia.gov/imrl/XWEB1128/xxtal.htm.

[10] J. Bovatsek, L. Shah, A. Arai, and Y. Uehara: 5th Int. Symp. on Laser Precision Microfabrication, Proc. of SPIE Vol. 5662 (2004) p.661.

[11] J.M. Bovatsek, F. Yoshino, and A.Y. Arai: Proc. 6th Int. Symp. on Laser Precision Microfabrication (2005) 05-1.

[12] A.M. Streltsov, and N.F. Borrelli, J. Opt. Soc. Am. B, **19**, (2002) 2496.

[13] M. Scheik-Bahae, D.C. Hutchings, D.J. Hagan, and E.W. Van Stryland: IEEE J. Quantum Electron. **27**, (1991) 1296.

[14] E. Mazur "Laser Applications in Microelectronic and Optoelectronic Manufacturing XI", Proc. of SPIE Vol. 6106A-19 (2006).

[15] T.H.R. Crawford, A. Borowiec, and H.K. Haugan: CLEO/QELS Conference Technical Digest, (2003) CFF6.

[16] H. K. Tonshoff, A. Ostendorf, and T. Wagner: Laser Application in Microelectronics and Optoelectronic Manufacturing VI, Proc. of SPIE Vol. 4274 (2001) 88.

[17] A. Major, F. Yoshino, I. Nikolakakos, J.S. Aitchison, and P. W. E. Smith: Opt. Lett., **29**, (2004) 602.

[18] http://www.miyachi-gr.co.jp/pro/maker/laser/ml9000a.html.

[19] J. Bonse, S. Baudach, J. Kruger, W. Kautek: "High-Power Laser Ablation III", Proc. of SPIE Vol. 4065 (2000) p.161.

(Received: May 16, 2006, Accepted: December 1, 2006)